J. DIFERENSIAL/E-ISSN:2775-9644
Vol.8(2),2026, 219–241
doi:https://doi.org/10.35508/jd.v8i2.29098

RESEARCH ARTICLE

A Caputo–Fabrizio Fractional-Order Typhoid Fever Model with Environmental Transmission and Sensitivity Analysis

El-mahdi Nafia[1,*], Ali Es-sallamy[1], M'hamed El Omari[1]

[1]*Laboratory of Applied Mathematics and Scientific Computing, Sultan Moulay Slimane University, PO Box 532, Beni Mellal, 23000, Morocco*
[*]*Corresponding author: El-mahdi Nafia, nafia.el-mahdi@usms.ac.ma*

Received: 23 June 2026; Revised: 15 September 2026; Accepted: 11 October 2026; Published: 7 November 2026.

Abstract:
This paper presents a Caputo–Fabrizio fractional-order model for typhoid fever transmission with environmental contamination. The model incorporates vaccination, symptomatic and asymptomatic infections, hospitalization, recovery, immigration, and bacterial persistence in contaminated water and food. The positivity, boundedness, and positive invariance of the feasible region are established. The existence and uniqueness of solutions are proved using the Banach fixed-point theorem. The disease-free equilibrium and the basic reproduction number $\mathcal{R}_0$ are derived by the next-generation matrix method. A sensitivity analysis of $\mathcal{R}_0$ identifies the key parameters influencing disease spread. Numerical simulations for different fractional orders show that the fractional order modifies the transient dynamics of the infected classes and the environmental bacterial load. These simulations are interpreted as qualitative, literature-informed model outputs; in the absence of statistical calibration and independent validation, they do not establish that the Caputo–Fabrizio formulation provides a superior fit or predictive performance relative to the integer-order model.

Keywords: Typhoid fever; Caputo–Fabrizio fractional derivative; mathematical modeling; environmental transmission; basic reproduction number; existence and uniqueness; sensitivity analysis; numerical simulation

1. Introduction

Typhoid fever, also known as enteric fever, is a serious infectious disease caused mainly by *Salmonella enterica* serovar Typhi, while *Salmonella* Paratyphi A, B, and C may also cause enteric fever [1, 2]. The disease remains a major public health concern, particularly in regions where access to clean water, adequate sanitation, and effective medical care is limited. Unlike many non-typhoidal *Salmonella* infections, which usually cause localized gastrointestinal symptoms, typhoid fever may involve both the intestinal tract and the bloodstream. Its transmission occurs primarily through ingestion of contaminated food or water, which makes environmental contamination an essential factor in the persistence and spread of the disease [3, 4].

The clinical progression of typhoid fever is strongly influenced by the bacterial load, host immunity, stomach acidity, and the presence of asymptomatic carriers [5, 6]. The incubation period is usually between 10 and 20 days, although it may vary depending on the infectious dose and individual

© Nafia *et al.*

health conditions [4]. Symptomatic infected individuals may present with fever, fatigue, abdominal discomfort, and other nonspecific symptoms, whereas asymptomatic carriers can continue to shed bacteria into the environment without showing clinical signs. This hidden transmission route increases the difficulty of disease control and highlights the need for mathematical models that include both symptomatic and asymptomatic infections [7, 8].

Despite progress in diagnosis, treatment, vaccination, and public health interventions, typhoid fever continues to impose a considerable global burden. Recent studies have reported millions of enteric fever cases worldwide, with a significant number of deaths, particularly among children and vulnerable populations [9, 10]. Moreover, the emergence of antimicrobial-resistant *Salmonella* strains has made treatment more difficult and has increased the importance of preventive strategies such as vaccination, hygiene education, water disinfection, and food sterilization [2, 11, 12]. Currently, several types of typhoid vaccines are available, including typhoid conjugate vaccines, Vi polysaccharide vaccines, and Ty21a oral vaccines. Nevertheless, vaccination alone may not be sufficient in highly endemic regions where sanitation and environmental contamination remain major drivers of transmission [13].

Mathematical modeling has become an important tool for understanding the transmission dynamics of typhoid fever and for evaluating control strategies. Several deterministic models have been developed to describe direct human-to-human transmission, indirect transmission through contaminated food or water, and hybrid transmission mechanisms combining both pathways [14–16]. Other studies have focused on the role of treatment, screening, sanitation, public health education, media awareness, and vaccination in reducing typhoid prevalence [18–24]. For example, Tilahun et al. [23] investigated typhoid fever control using cost-effective strategies, while Musa et al. [21] emphasized the role of public health education programs. Alharbi et al. [25] analyzed a periodic typhoid model with imperfect vaccination, treatment, and water sanitation. These studies demonstrate the importance of combining vaccination, treatment, hygiene awareness, and environmental sanitation in typhoid modeling.

More recently, Oubouskour et al. [27] proposed a deterministic mathematical model for typhoid fever transmission in Taiwan. Their model incorporates susceptible individuals, vaccinated susceptible individuals, exposed individuals, symptomatic infected individuals, asymptomatic infected individuals, hospitalized or treated individuals, recovered individuals, and an environmental bacterial compartment. The model also considers infected immigrants, population and hospital waste contamination, treatment discontinuation, and different public health interventions. Using optimal control theory and cost-effectiveness analysis, they showed that combined strategies, especially awareness campaigns and vaccination programs, can substantially reduce the disease burden.

Fractional typhoid modeling predates the present study. Shaikh and Nisar [17] formulated a Caputo–Fabrizio typhoid model and studied existence, uniqueness, stability, and numerical approximation. Abboubakar et al. [26] subsequently developed a non-integer-order typhoid model with vaccination, stability analysis, sensitivity analysis, and calibration to clinical data from Mbandjock. Accordingly, the present paper does not claim the first use of fractional calculus, or of the Caputo–Fabrizio operator, for typhoid fever.

Classical integer-order epidemic models do not explicitly encode history dependence in the time derivative. Fractional calculus provides one mathematical framework for examining memory-dependent dynamics in which the current state may depend on previous exposure, contamination, treatment history, or delayed behavioral response [28–30]. In particular, the Caputo–Fabrizio derivative uses a non-singular exponential kernel and therefore provides a convenient framework for representing exponentially fading memory effects [31, 32]. This modeling choice is not, by itself, evidence of greater biological realism or predictive accuracy; such claims require calibration and validation against epidemiological data.

Fractional-order epidemic models have been widely used in recent years to examine the dynamics of several infectious diseases. Ahmed et al. [33] studied a Caputo fractional-order diphtheria model and established existence, uniqueness, and sensitivity results. Alkahtani [29] used a fractional-order derivative to model COVID-19 transmission. Yusuf et al. [34] investigated pine wilt disease using a Caputo fractional operator, while Jan et al. [35] modeled dengue transmission through fractional derivatives. Ullah et al. [36] developed a Caputo–Fabrizio fractional-order vector-borne disease model and studied its equilibrium points, basic reproduction number, existence and uniqueness of solutions, sensitivity analysis, and numerical simulations. These studies show that fractional operators provide an additional modeling degree of freedom for studying memory-dependent transient behavior; whether they improve agreement with observed data is a separate empirical question.

Motivated by these works, the present paper develops a Caputo–Fabrizio extension of the detailed deterministic typhoid model of Oubouskour et al. [27]. The model retains eight epidemiological states: susceptible individuals $S(t)$, vaccinated susceptible individuals $S_v(t)$, exposed individuals $E(t)$, symptomatic infected individuals $I_S(t)$, asymptomatic infected individuals $I_A(t)$, hospitalized individuals $H(t)$, recovered individuals $R(t)$, and a scaled environmental bacterial load $E_n(t)$. Thus, unlike the earlier Caputo–Fabrizio typhoid model of Shaikh and Nisar [17], the present framework simultaneously resolves vaccination, latent infection, symptomatic/asymptomatic progression, hospitalization, recovery, and an explicit environmental bacterial load within the same fractional system.

The contribution is therefore not the first application of the Caputo–Fabrizio operator to typhoid fever. Rather, it is the formulation and analysis of this more detailed transmission structure within a consistently initialized Caputo–Fabrizio integral framework. We establish local existence and uniqueness, positivity, boundedness, and positive invariance; derive the disease-free equilibrium and $\mathcal{R}_0$; justify the Caputo–Fabrizio linear stability criterion at the disease-free state; recompute normalized forward sensitivity indices at a common literature-informed baseline; and assess the numerical scheme by time-step refinement. The simulations are used only to examine how the fractional order changes transient model behavior and are not interpreted as evidence of superior fit or predictive accuracy.

The remainder of this paper is organized as follows. Section 2 presents the basic preliminaries of fractional calculus and introduces the Caputo–Fabrizio derivative. Section 3 formulates the fractional-order typhoid fever model and studies its qualitative properties, including positivity, boundedness, existence, uniqueness, the disease-free equilibrium, and the basic reproduction number. Section 4 presents the sensitivity analysis of $\mathcal{R}_0$. Section 5 provides numerical simulations and a graphical discussion for different fractional orders. Finally, Section 6 concludes the paper and highlights possible directions for future research.

2. Preliminaries

This section recalls the Caputo–Fabrizio fractional derivative and its associated integral operator, which are used in the analysis of the proposed model. The Caputo–Fabrizio derivative was introduced in [40] as a fractional derivative with a non-singular exponential kernel. Some important properties of this operator and its corresponding fractional integral were further discussed in [41].

Definition 2.1. [40, 41] Let $g \in H^1(0,T)$, where $T > 0$, and let $0 < \alpha < 1$. We use the Losada–Nieto normalization of the Caputo–Fabrizio derivative,

$$ {}^{CF}D_t^{\alpha} g(t) = \frac{1}{1-\alpha} \int_0^t g'(\xi) \exp\left[-\frac{\alpha}{1-\alpha}(t-\xi)\right] d\xi. \tag{2.1}$$

This corresponds to $M(\alpha) = 2/(2-\alpha)$ in the general Caputo–Fabrizio normalization.

Definition 2.2. [40, 41] For a continuous function ψ, the associated Caputo–Fabrizio integral is

$$ {}^{CF}I_t^{\alpha}\psi(t) = (1-\alpha)\psi(t) + \alpha \int_0^t \psi(y)\, dy, \qquad 0 < \alpha < 1. \tag{2.2}$$

Hence the derivative and integral operators used in the sequel belong to the same normalization.

Lemma 2.1 (Initialized Caputo–Fabrizio integral representation). *[37] Let $\psi : [0, b] \to \mathbb{R}$ be continuous and $x_0 \in \mathbb{R}$. For arbitrary prescribed initial data, we use the initialized integral formulation*

$$ x(t) = x_0 + (1-\alpha)\big[\psi(t) - \psi(0)\big] + \alpha \int_0^t \psi(y)\, dy. \tag{2.3}$$

It satisfies $x(0) = x_0$ exactly.

Remark 1 (Initial-time compatibility). Because the kernel in (2.1) is bounded, ${}^{CF}D_t^{\alpha}x(0) = 0$ for sufficiently regular x. Thus, a strict differential initial-value problem ${}^{CF}D_t^{\alpha}x(t) = \psi(t)$ imposed also at $t = 0$ requires the compatibility condition $\psi(0) = 0$. Epidemiological initial states need not satisfy this restriction. To make the initialization unambiguous, the existence, uniqueness, and numerical parts of this paper are therefore formulated through (2.3). When $\psi(0) = 0$ (in particular in equilibrium-based linearization), this reduces to the standard Caputo–Fabrizio integral relation.

When $\alpha \to 1$, the initialized integral formulation formally reduces to the corresponding classical first-order integral equation.

3. Caputo–Fabrizio Fractional Typhoid Fever Model

The total population is divided into eight compartments:

$$ S(t), \quad S_v(t), \quad E(t), \quad I_S(t), \quad I_A(t), \quad H(t), \quad R(t), \quad E_n(t), $$

where S, S_v, E, I_S, I_A, H, and R denote, respectively, susceptible, vaccinated susceptible, exposed, symptomatic infected, asymptomatic infected, hospitalized, and recovered individuals. The variable E_n represents a scaled environmental bacterial load associated with contaminated water and food. Because the available sources do not specify a sampling volume or a CFU-based calibration for this compartment, E_n is expressed in scaled load units rather than interpreted as a measured concentration.

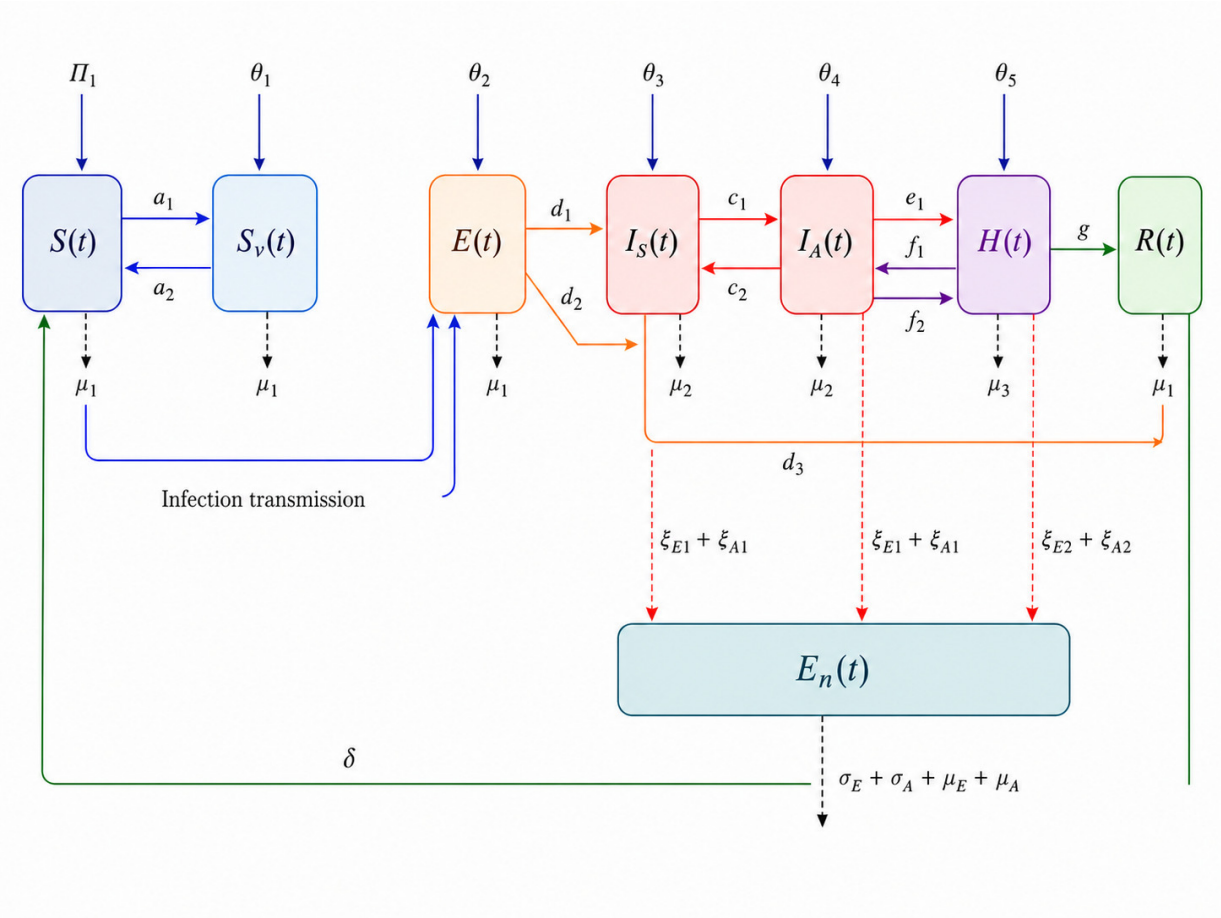


Figure 3.1: Schematic representation of the proposed Caputo–Fabrizio fractional-order typhoid fever model.

The schematic flow of the model is shown in Figure 3.1. The Caputo–Fabrizio fractional-order typhoid fever model is given by

$$
\begin{cases}
{}^{CF}D_t^{\alpha} S(t) = \Pi_1 + a_2 S_v(t) + \delta R(t) - (\mu_1 + a_1) S(t) - [b_1 I_S(t) + b_2 I_A(t) + (\beta_{E1} + \beta_{A1}) E_n(t)]\, S(t), \\
{}^{CF}D_t^{\alpha} S_v(t) = \theta_1 - (a_2 + \mu_1) S_v(t) + a_1 S(t) - [b_1' I_S(t) + b_2' I_A(t) + (\beta_{E2} + \beta_{A2}) E_n(t)]\, S_v(t), \\
{}^{CF}D_t^{\alpha} E(t) = \theta_2 - (\mu_1 + \lambda_1 + d_1 + d_2 + d_3) E(t) + [b_1 I_S(t) + b_2 I_A(t) + (\beta_{E1} + \beta_{A1}) E_n(t)]\, S(t) \\
\qquad\qquad + [b_1' I_S(t) + b_2' I_A(t) + (\beta_{E2} + \beta_{A2}) E_n(t)]\, S_v(t), \\
{}^{CF}D_t^{\alpha} I_S(t) = \theta_3 + d_1 E(t) + c_2 I_A(t) - (c_1 + e_1 + \lambda_2 + \mu_1 + \mu_2) I_S(t) + f_1 H(t), \\
{}^{CF}D_t^{\alpha} I_A(t) = \theta_4 + d_2 E(t) + c_1 I_S(t) - (c_2 + e_2 + \lambda_3 + \mu_1 + \mu_3) I_A(t) + f_2 H(t), \\
{}^{CF}D_t^{\alpha} H(t) = \theta_5 + e_1 I_S(t) + e_2 I_A(t) - (g + \lambda_4 + \mu_1 + \mu_2 + f_1 + f_2) H(t), \\
{}^{CF}D_t^{\alpha} R(t) = g H(t) + d_3 E(t) - (\mu_1 + \delta) R(t), \\
{}^{CF}D_t^{\alpha} E_n(t) = -(\sigma_E + \sigma_A + \mu_E + \mu_A) E_n(t) + (\xi_{E1} + \xi_{A1})(I_A(t) + I_S(t)) + (\xi_{E2} + \xi_{A2}) H(t).
\end{cases}
\tag{3.1}
$$

The initial conditions are

$$
S(0) = S^0 \geq 0, \quad S_v(0) = S_v^0 \geq 0, \quad E(0) = E^0 \geq 0, \quad I_S(0) = I_S^0 \geq 0,
$$

$$
I_A(0) = I_A^0 \geq 0, \quad H(0) = H^0 \geq 0, \quad R(0) = R^0 \geq 0, \quad E_n(0) = E_n^0 \geq 0.
$$

The total human population is

$$N(t) = S(t) + S_v(t) + E(t) + I_S(t) + I_A(t) + H(t) + R(t).$$

The infection terms are defined by

$$\Delta_1 = [b_1 I_S(t) + b_2 I_A(t) + (\beta_{E1} + \beta_{A1}) E_n(t)]\, S(t),$$

and

$$\Delta_2 = \left[b_1' I_S(t) + b_2' I_A(t) + (\beta_{E2} + \beta_{A2}) E_n(t)\right] S_v(t).$$

Thus, the exposed class receives new infections from susceptible and vaccinated susceptible individuals through direct and environmental transmission.

Table 3.1: Meaning of variables and parameters of the fractional typhoid fever model.

Variable/Parameter	Meaning
$S(t)$	Susceptible individuals
$S_v(t)$	Vaccinated susceptible individuals
$E(t)$	Exposed individuals
$I_S(t)$	Symptomatic infected individuals
$I_A(t)$	Asymptomatic infected individuals
$H(t)$	Hospitalized or treated individuals
$R(t)$	Recovered individuals
$E_n(t)$	Scaled environmental bacterial load associated with contaminated water and food
α	Fractional derivative order, $0 < \alpha < 1$; $\alpha = 1$ gives the classical case
Π_1	Birth rate of newborns entering the population
θ_1	Immigration rate of vaccinated individuals
θ_2	Immigration rate of individuals carrying *Salmonella* bacteria
θ_3	Immigration rate of symptomatic infected individuals
θ_4	Immigration rate of asymptomatic infected individuals
θ_5	Immigration rate of treated individuals
λ_1	Exit rate of individuals carrying *Salmonella*
λ_2	Exit rate of symptomatic infected individuals
λ_3	Exit rate of asymptomatic infected individuals
λ_4	Exit rate of treated individuals
μ_1	Natural mortality rate
μ_2	Disease-induced mortality rate for symptomatic infected individuals
μ_3	Disease-induced mortality rate for asymptomatic infected individuals
μ_E	Bacterial mortality rate in water
μ_A	Bacterial mortality rate in food
σ_E	Water disinfection rate
σ_A	Food disinfection rate
β_{E1}	Transmission rate from contaminated water to susceptible individuals
β_{A1}	Transmission rate from contaminated food to susceptible individuals
β_{E2}	Transmission rate from contaminated water to vaccinated susceptible individuals
β_{A2}	Transmission rate from contaminated food to vaccinated susceptible individuals
a_1	Vaccination rate
a_2	Waning rate of vaccine-induced immunity
b_1	Transmission rate from symptomatic infected individuals to susceptible individuals
b_2	Transmission rate from asymptomatic infected individuals to susceptible individuals
b_1'	Transmission rate from symptomatic infected individuals to vaccinated susceptible individuals
b_2'	Transmission rate from asymptomatic infected individuals to vaccinated susceptible individuals
d_1	Progression rate from exposed to symptomatic infected individuals
d_2	Progression rate from exposed to asymptomatic infected individuals
d_3	Natural recovery rate from exposed class

Variable/Parameter	Meaning
c_1	Transition rate from symptomatic to asymptomatic infection
c_2	Transition rate from asymptomatic to symptomatic infection
e_1	Hospitalization rate of symptomatic infected individuals
e_2	Hospitalization rate of asymptomatic infected individuals
f_1	Treatment cessation rate from hospitalized class to symptomatic class
f_2	Treatment discontinuation or resistance rate from hospitalized class to asymptomatic class
g	Recovery rate of treated individuals
δ	Immunity loss rate
ξ_{E1}	Bacterial shedding rate in water by infected individuals
ξ_{A1}	Bacterial shedding rate in food by infected individuals
ξ_{E2}	Bacterial shedding rate in water by hospitalized individuals
ξ_{A2}	Bacterial shedding rate in food by hospitalized individuals

The model includes direct human-to-human transmission and indirect environmental transmission through contaminated food and water.

3.1. Analysis of the Caputo–Fabrizio Fractional Typhoid Model

Let $Q = [0, U]$ and let $Y(Q)$ be the Banach space of continuous real-valued functions on Q with the supremum norm. Set

$$\mathcal{N} = Y(Q)^8, \qquad X(t) = (S, S_v, E, I_S, I_A, H, R, E_n)^T, \qquad X_0 = X(0).$$

The model is autonomous, and its right-hand side is denoted by

$$\Psi(X) = (\psi_1(X), \dots, \psi_8(X))^T.$$

Following the initialization convention of Section 2, the evolution problem used in the well-posedness analysis is

$$X(t) = X_0 + (1-\alpha)\big[\Psi(X(t)) - \Psi(X_0)\big] + \alpha \int_0^t \Psi(X(y))\, dy. \tag{3.2}$$

In particular, (3.2) gives $X(0) = X_0$ for arbitrary non-negative epidemiological initial data.

For $R > 0$, define

$$\mathcal{B}_R = \big\{X \in C([0,U];\mathbb{R}^8) : X(0) = X_0,\ \|X - X_0\|_\infty \le R\big\}$$

and $K_R = \{z \in \mathbb{R}^8 : \|z - X_0\| \le R\}$. Since Ψ is polynomial in the state variables, it is continuous and locally Lipschitz. Hence there exist finite constants $L_R, M_R > 0$ satisfying

$$\|\Psi(z) - \Psi(w)\| \le L_R \|z - w\|, \qquad M_R = \sup_{z \in K_R} \|\Psi(z)\|. \tag{3.3}$$

Define

$$(\mathcal{T}X)(t) = X_0 + (1-\alpha)\big[\Psi(X(t)) - \Psi(X_0)\big] + \alpha \int_0^t \Psi(X(y))\, dy. \tag{3.4}$$

Theorem 3.1 (Local existence and uniqueness). *Let $X_0 \in \mathbb{R}^8_+$ and $0 < \alpha < 1$. Assume that $R, U > 0$ satisfy*

$$(1-\alpha) L_R R + \alpha U M_R \le R \tag{3.5}$$

and

$$q_R := L_R\big[(1-\alpha) + \alpha U\big] < 1. \tag{3.6}$$

Then (3.2) has a unique solution in $\mathcal{B}_R$ on $[0, U]$.

Proof. For $X \in \mathcal{B}_R$, (3.3) gives

$$\begin{aligned}\|(\mathcal{T}X)(t) - X_0\| &\le (1-\alpha)\|\Psi(X(t)) - \Psi(X_0)\| + \alpha \int_0^t \|\Psi(X(y))\|\, dy \\ &\le (1-\alpha)L_R R + \alpha U M_R \le R.\end{aligned}$$

Also $(\mathcal{T}X)(0) = X_0$, so $\mathcal{T}(\mathcal{B}_R) \subset \mathcal{B}_R$. For $X, Y \in \mathcal{B}_R$,

$$\begin{aligned}\|(\mathcal{T}X)(t) - (\mathcal{T}Y)(t)\| &\le (1-\alpha)L_R\|X(t) - Y(t)\| \\ &\quad + \alpha L_R \int_0^t \|X(y) - Y(y)\|\, dy \\ &\le q_R \|X - Y\|_\infty.\end{aligned}$$

Taking the supremum over $t \in [0, U]$ proves that $\mathcal{T}$ is a contraction. Banach's fixed-point theorem yields a unique fixed point in $\mathcal{B}_R$. □

3.2. Positivity of Solutions

Theorem 3.2. *If all initial conditions are non-negative, then every solution of system (3.1) remains non-negative throughout its interval of existence.*

Proof. Evaluating the right-hand side of system (3.1) on the boundary of the non-negative orthant gives

$$\begin{cases} {}^{CF}D_t^\alpha S(t)\big|_{S=0} = \Pi_1 + a_2 S_v + \delta R \ge 0, \\ {}^{CF}D_t^\alpha S_v(t)\big|_{S_v=0} = \theta_1 + a_1 S \ge 0, \\ {}^{CF}D_t^\alpha E(t)\big|_{E=0} = \theta_2 + \Delta_1 + \Delta_2 \ge 0, \\ {}^{CF}D_t^\alpha I_S(t)\big|_{I_S=0} = \theta_3 + d_1 E + c_2 I_A + f_1 H \ge 0, \\ {}^{CF}D_t^\alpha I_A(t)\big|_{I_A=0} = \theta_4 + d_2 E + c_1 I_S + f_2 H \ge 0, \\ {}^{CF}D_t^\alpha H(t)\big|_{H=0} = \theta_5 + e_1 I_S + e_2 I_A \ge 0, \\ {}^{CF}D_t^\alpha R(t)\big|_{R=0} = gH + d_3 E \ge 0, \\ {}^{CF}D_t^\alpha E_n(t)\big|_{E_n=0} = (\xi_{E1} + \xi_{A1})(I_A + I_S) + (\xi_{E2} + \xi_{A2})H \ge 0. \end{cases}$$

Thus, the epidemiological vector field is quasi-positive on the boundary of $\mathbb{R}^8_+$. Using the comparison principle for Caputo–Fabrizio epidemic systems (see, e.g., [38]), the componentwise boundary inequalities above imply that a trajectory starting from non-negative data cannot cross a coordinate hyperplane toward negative values. Therefore

$$X(t) \in \mathbb{R}^8_+, \qquad t \in [0, U].$$

□

3.3. Boundedness and Positive Invariance

Theorem 3.3. *Assume $\mu_1 > 0$ and $q_{10} = \sigma_E + \sigma_A + \mu_E + \mu_A > 0$. Define*

$$Z = \Pi_1 + \theta_1 + \theta_2 + \theta_3 + \theta_4 + \theta_5, \qquad B_N = \max\left\{N(0), \frac{Z}{\mu_1}\right\},$$

$$C_E = B_N\left[2(\xi_{E1} + \xi_{A1}) + (\xi_{E2} + \xi_{A2})\right], \qquad B_E = \max\left\{E_n(0), \frac{C_E}{q_{10}}\right\}.$$

Then

$$\Omega = \{X \in \mathbb{R}^8_+ : 0 \le N \le B_N,\ 0 \le E_n \le B_E\}$$

is positively invariant along every solution throughout its interval of existence.

Proof. Adding the first seven state equations gives

$$\begin{aligned} {}^{CF}D_t^{\alpha} N(t) &= Z - \mu_1 N(t) - \lambda_1 E(t) - (\lambda_2 + \mu_2) I_S(t) \\ &\quad - (\lambda_3 + \mu_3) I_A(t) - (\lambda_4 + \mu_2) H(t) \\ &\leq Z - \mu_1 N(t). \end{aligned}$$

The constant B_N is a supersolution since ${}^{CF}D_t^{\alpha} B_N = 0 \geq Z - \mu_1 B_N$, and $N(0) \leq B_N$. The Caputo–Fabrizio comparison principle therefore yields

$$0 \leq N(t) \leq B_N.$$

Moreover,

$${}^{CF}D_t^{\alpha} E_n(t) = -q_{10} E_n(t) + (\xi_{E1} + \xi_{A1})(I_A + I_S) + (\xi_{E2} + \xi_{A2}) H.$$

Since $I_A, I_S, H \leq N \leq B_N$,

$${}^{CF}D_t^{\alpha} E_n(t) \leq -q_{10} E_n(t) + C_E.$$

The constant B_E satisfies ${}^{CF}D_t^{\alpha} B_E = 0 \geq -q_{10} B_E + C_E$ and $E_n(0) \leq B_E$. A second comparison gives

$$0 \leq E_n(t) \leq B_E.$$

Together with positivity, this proves the positive invariance of Ω. □

3.4. Disease-Free Steady State

The disease-free steady state corresponds to the absence of typhoid infection. Thus,

$$E = I_S = I_A = H = R = E_n = 0.$$

To obtain a true disease-free equilibrium, we assume that there is no infected immigration, namely

$$\theta_2 = \theta_3 = \theta_4 = \theta_5 = 0.$$

At the disease-free equilibrium, the first two equations of system (3.1) give

$$\Pi_1 + a_2 S_v - (\mu_1 + a_1) S = 0,$$

and

$$\theta_1 - (a_2 + \mu_1) S_v + a_1 S = 0.$$

Equivalently,

$$(\mu_1 + a_1) S - a_2 S_v = \Pi_1,$$

and

$$-a_1 S + (a_2 + \mu_1) S_v = \theta_1.$$

Let

$$D = (\mu_1 + a_1)(a_2 + \mu_1) - a_1 a_2 = \mu_1(\mu_1 + a_1 + a_2).$$

Then

$$S^0 = \frac{\Pi_1 (a_2 + \mu_1) + a_2 \theta_1}{D}, \tag{3.7}$$

and

$$S_v^0 = \frac{(\mu_1 + a_1)\theta_1 + a_1 \Pi_1}{D}. \tag{3.8}$$

Hence, the disease-free equilibrium is

$$\mathcal{E}_0 = (S^0, S_v^0, 0, 0, 0, 0, 0, 0), \tag{3.9}$$

where S^0 and S_v^0 are given by (3.7) and (3.8).

3.5. Basic Reproduction Number

The basic reproduction number $\mathcal{R}_0$ is computed using the next-generation matrix method. We consider the infected compartments

$$x = (E, I_S, I_A, H, E_n)^T.$$

Let

$$\begin{aligned} q_3 &= \mu_1 + \lambda_1 + d_1 + d_2 + d_3, \\ q_4 &= c_1 + e_1 + \lambda_2 + \mu_1 + \mu_2, \\ q_5 &= c_2 + e_2 + \lambda_3 + \mu_1 + \mu_3, \\ q_6 &= g + \lambda_4 + \mu_1 + \mu_2 + f_1 + f_2, \end{aligned}$$

and

$$q_{10} = \sigma_E + \sigma_A + \mu_E + \mu_A.$$

Also, define

$$q_8 = \xi_{E1} + \xi_{A1}, \qquad q_9 = \xi_{E2} + \xi_{A2}.$$

For simplicity, set

$$\begin{aligned} k_S &= b_1 S^0 + b_1' S_v^0, \\ k_A &= b_2 S^0 + b_2' S_v^0, \end{aligned}$$

and

$$k_E = (\beta_{E1} + \beta_{A1}) S^0 + (\beta_{E2} + \beta_{A2}) S_v^0.$$

The matrix of new infection terms is

$$F = \begin{pmatrix} 0 & k_S & k_A & 0 & k_E \\ 0 & 0 & 0 & 0 & 0 \\ 0 & 0 & 0 & 0 & 0 \\ 0 & 0 & 0 & 0 & 0 \\ 0 & 0 & 0 & 0 & 0 \end{pmatrix}.$$

The transition matrix is

$$V = \begin{pmatrix} q_3 & 0 & 0 & 0 & 0 \\ -d_1 & q_4 & -c_2 & -f_1 & 0 \\ -d_2 & -c_1 & q_5 & -f_2 & 0 \\ 0 & -e_1 & -e_2 & q_6 & 0 \\ 0 & -q_8 & -q_8 & -q_9 & q_{10} \end{pmatrix}.$$

Therefore, the basic reproduction number is

$$\mathcal{R}_0 = \rho(FV^{-1}), \tag{3.10}$$

where $\rho(\cdot)$ denotes the spectral radius.

Equivalently, let $Y = (Y_1, Y_2, Y_3)^T$ be the solution of

$$\begin{pmatrix} q_4 & -c_2 & -f_1 \\ -c_1 & q_5 & -f_2 \\ -e_1 & -e_2 & q_6 \end{pmatrix} \begin{pmatrix} Y_1 \\ Y_2 \\ Y_3 \end{pmatrix} = \frac{1}{q_3} \begin{pmatrix} d_1 \\ d_2 \\ 0 \end{pmatrix}.$$

The environmental contribution is

$$Y_4 = \frac{q_8(Y_1 + Y_2) + q_9 Y_3}{q_{10}}.$$

Thus,

$$\mathcal{R}_0 = k_S Y_1 + k_A Y_2 + k_E Y_4. \tag{3.11}$$

That is,

$$\mathcal{R}_0 = (b_1 S^0 + b_1' S_v^0) Y_1 + (b_2 S^0 + b_2' S_v^0) Y_2 + \left[(\beta_{E1} + \beta_{A1}) S^0 + (\beta_{E2} + \beta_{A2}) S_v^0 \right] Y_4.$$

Theorem 3.4. *The disease-free equilibrium $\mathcal{E}_0$ is locally asymptotically stable if $\mathcal{R}_0 < 1$ and unstable if $\mathcal{R}_0 > 1$.*

Proof. Let $x = (E, I_S, I_A, H, E_n)^T$. Linearization at $\mathcal{E}_0$ gives

$${}^{CF}D_t^{\alpha} x(t) = (F - V)x(t).$$

Write

$$V = \begin{pmatrix} V_h & 0 \\ -r^T & q_{10} \end{pmatrix}, \qquad r^T = (0, q_8, q_8, q_9),$$

where V_h is the upper-left 4×4 block. The matrix V_h is a Z-matrix and is strictly column diagonally dominant because

$$q_3 > d_1 + d_2, \qquad q_4 > c_1 + e_1, \qquad q_5 > c_2 + e_2, \qquad q_6 > f_1 + f_2.$$

Hence V_h is a nonsingular M-matrix and $V_h^{-1} \geq 0$. Since $q_{10} > 0$,

$$V^{-1} = \begin{pmatrix} V_h^{-1} & 0 \\ q_{10}^{-1} r^T V_h^{-1} & q_{10}^{-1} \end{pmatrix} \geq 0.$$

Thus V is a nonsingular M-matrix. By the next-generation matrix criterion, $\mathcal{R}_0 = \rho(FV^{-1}) < 1$ implies that $A := F - V$ is Hurwitz.

For the normalized linear Caputo–Fabrizio system ${}^{CF}D_t^{\alpha} z = Az$, the characteristic matrix is [39]

$$s\big(I - (1-\alpha)A\big) - \alpha A.$$

Accordingly, an eigenvalue λ of A produces the temporal exponent

$$\omega_\alpha(\lambda) = \frac{\alpha\lambda}{1 - (1-\alpha)\lambda}. \tag{3.12}$$

If $\lambda = a + ib$, then

$$\Re\,\omega_\alpha(\lambda) = \alpha \frac{a - (1-\alpha)|\lambda|^2}{|1 - (1-\alpha)\lambda|^2}.$$

Therefore $\Re\lambda < 0$ implies $\Re\,\omega_\alpha(\lambda) < 0$. The denominator cannot vanish in the left half-plane because $1/(1-\alpha) > 0$. Hence every linearized CF mode decays when A is Hurwitz, proving local asymptotic stability for $\mathcal{R}_0 < 1$. If $\mathcal{R}_0 > 1$, the infected linearization is unstable, and so is $\mathcal{E}_0$. □

3.6. Endemic Equilibrium

The endemic equilibrium is denoted by

$$\mathcal{E}^* = (S^*, S_v^*, E^*, I_S^*, I_A^*, H^*, R^*, E_n^*),$$

where

$$E^* > 0, \quad I_S^* > 0, \quad I_A^* > 0, \quad H^* > 0, \quad E_n^* > 0.$$

At equilibrium, $\mathcal{E}^*$ satisfies the algebraic system

$$\begin{cases} 0 = \Pi_1 + a_2 S_v^* + \delta R^* - (\mu_1 + a_1) S^* - [b_1 I_S^* + b_2 I_A^* + (\beta_{E1} + \beta_{A1}) E_n^*]\, S^*, \\ 0 = \theta_1 - (a_2 + \mu_1) S_v^* + a_1 S^* - [b_1' I_S^* + b_2' I_A^* + (\beta_{E2} + \beta_{A2}) E_n^*]\, S_v^*, \\ 0 = \theta_2 - q_3 E^* + [b_1 I_S^* + b_2 I_A^* + (\beta_{E1} + \beta_{A1}) E_n^*]\, S^* \\ \qquad\qquad + [b_1' I_S^* + b_2' I_A^* + (\beta_{E2} + \beta_{A2}) E_n^*]\, S_v^*, \\ 0 = \theta_3 + d_1 E^* + c_2 I_A^* - q_4 I_S^* + f_1 H^*, \\ 0 = \theta_4 + d_2 E^* + c_1 I_S^* - q_5 I_A^* + f_2 H^*, \\ 0 = \theta_5 + e_1 I_S^* + e_2 I_A^* - q_6 H^*, \\ 0 = g H^* + d_3 E^* - (\mu_1 + \delta) R^*, \\ 0 = -q_{10} E_n^* + q_8 (I_A^* + I_S^*) + q_9 H^*. \end{cases} \tag{3.13}$$

From the seventh and eighth equations, we obtain

$$R^* = \frac{g H^* + d_3 E^*}{\mu_1 + \delta},$$

and

$$E_n^* = \frac{q_8 (I_A^* + I_S^*) + q_9 H^*}{q_{10}}.$$

The remaining components

$$S^*, \quad S_v^*, \quad E^*, \quad I_S^*, \quad I_A^*, \quad H^*$$

are obtained by solving the first six algebraic equations of (3.13). Due to the coupling between direct transmission, environmental contamination, hospitalization, recovery, and loss of immunity, an explicit closed-form expression is difficult to obtain.

Therefore, in this work, the endemic equilibrium is characterized as a positive solution of the steady-state algebraic system (3.13). A complete proof of existence and uniqueness of $\mathcal{E}^*$ is left for future investigation.

4. Sensitivity Index with Respect to $\mathcal{R}_0$

In this section, we evaluate the local influence of selected epidemiological parameters on the basic reproduction number $\mathcal{R}_0$. For a parameter ζ, the normalized forward sensitivity index is

$$\Pi_\zeta^{\mathcal{R}_0} = \frac{\zeta}{\mathcal{R}_0} \frac{\partial \mathcal{R}_0}{\partial \zeta}. \tag{4.1}$$

Thus, $\Pi_\zeta^{\mathcal{R}_0} > 0$ means that a local increase in ζ increases $\mathcal{R}_0$, whereas $\Pi_\zeta^{\mathcal{R}_0} < 0$ means that it decreases $\mathcal{R}_0$.

To evaluate all indices at one common and internally consistent point, we use a literature-informed disease-free baseline. For Taiwan, Alharbi et al. [25] report a population of $23{,}257{,}434$, a natural mortality rate $\mu_1 = 3.42081 \times 10^{-5}$ day^{-1}, and the corresponding recruitment rate $\Pi_1 = 795.592$ persons/day. Their baseline vaccine efficacy is $\varepsilon_v = 0.75$. We therefore use a closed disease-free reference scenario with

$$\theta_1 = \theta_2 = \theta_3 = \theta_4 = \theta_5 = 0,$$

and represent the reduced susceptibility of vaccinated individuals by

$$b_j' = (1 - \varepsilon_v) b_j, \qquad j = 1, 2,$$

$$\beta_{E2} = (1-\varepsilon_v)\beta_{E1}, \qquad \beta_{A2} = (1-\varepsilon_v)\beta_{A1}.$$

With $\varepsilon_v = 0.75$, this gives

$$b_1' = b_2' = 2.5 \times 10^{-9}, \qquad \beta_{E2} = \beta_{A2} = 2.5 \times 10^{-10}.$$

The remaining transition and environmental parameters are kept at the baseline values listed in Table 5.3. This baseline is used to obtain an internally consistent sensitivity calculation; it is not presented as a direct statistical calibration of the present fractional model.

Using (3.7)–(3.8), the corresponding disease-free susceptible populations are

$$S^0 = 8.168662 \times 10^6, \qquad S_v^0 = 1.508875 \times 10^7,$$

so that $S^0 + S_v^0 \approx 2.325742 \times 10^7$. Solving the linear system defining Y_1, Y_2, Y_3 in Section 3 gives

$$Y_1 = 1.715634, \qquad Y_2 = 0.660102, \qquad Y_3 = 4.507557,$$

and

$$Y_4 = 17.539679.$$

Substitution into (3.11) yields the baseline reproduction number

$$\mathcal{R}_0^{\text{base}} = 0.702560. \tag{4.2}$$

For parameters that enter (3.11) explicitly, the derivatives in (4.1) are evaluated analytically. For parameters that act through $Y = (Y_1, Y_2, Y_3)^T$, write the defining system as

$$B(\zeta)Y(\zeta) = r(\zeta).$$

Differentiation gives

$$\frac{\partial Y}{\partial \zeta} = B(\zeta)^{-1}\left(\frac{\partial r}{\partial \zeta} - \frac{\partial B}{\partial \zeta}Y\right). \tag{4.3}$$

The resulting indices were independently checked by the centered relative finite-difference formula

$$\Pi_{\zeta}^{\mathcal{R}_0} \approx \frac{\mathcal{R}_0(\zeta(1+\epsilon)) - \mathcal{R}_0(\zeta(1-\epsilon))}{2\epsilon\,\mathcal{R}_0(\zeta)}, \qquad \epsilon = 10^{-5}. \tag{4.4}$$

The analytical and finite-difference values agree to the displayed precision. For example,

$$\Pi_{b_1}^{\mathcal{R}_0} = \frac{b_1 S^0 Y_1}{\mathcal{R}_0}, \qquad \Pi_{b_2}^{\mathcal{R}_0} = \frac{b_2 S^0 Y_2}{\mathcal{R}_0},$$

and

$$\Pi_{\beta_{E1}}^{\mathcal{R}_0} = \frac{\beta_{E1} S^0 Y_4}{\mathcal{R}_0}, \qquad \Pi_{\beta_{A1}}^{\mathcal{R}_0} = \frac{\beta_{A1} S^0 Y_4}{\mathcal{R}_0}.$$

Consequently, parameters that enter $\mathcal{R}_0$ symmetrically and have identical baseline values necessarily have identical normalized indices. In particular,

$$\Pi_{\beta_{E1}}^{\mathcal{R}_0} = \Pi_{\beta_{A1}}^{\mathcal{R}_0}, \qquad \Pi_{\beta_{E2}}^{\mathcal{R}_0} = \Pi_{\beta_{A2}}^{\mathcal{R}_0}.$$

The same consistency holds for σ_E, σ_A and for μ_E, μ_A at equal baseline values.

Table 4.1: Literature-informed baseline values and normalized forward sensitivity indices of $\mathcal{R}_0$. All indices are evaluated at the common baseline $\mathcal{R}_0^{\text{base}} = 0.702560$.

Parameter	Baseline value	Sensitivity index	Local effect
b_1	1.0×10^{-8}	0.19948	Increase
b_2	1.0×10^{-8}	0.07675	Increase
b_1'	2.5×10^{-9}	0.09212	Increase
b_2'	2.5×10^{-9}	0.03544	Increase
β_{E1}	1.0×10^{-9}	0.20393	Increase
β_{A1}	1.0×10^{-9}	0.20393	Increase
β_{E2}	2.5×10^{-10}	0.09417	Increase
β_{A2}	2.5×10^{-10}	0.09417	Increase
σ_E	0.01	−0.02516	Decrease
σ_A	0.01	−0.02516	Decrease
μ_E	0.1085	−0.27295	Decrease
μ_A	0.1085	−0.27295	Decrease
e_1	0.375	−0.53205	Decrease
e_2	0.064	−0.08515	Decrease
g	0.0512	−0.07472	Decrease

Table 4.1 shows that the largest-magnitude local negative index in this baseline is associated with the hospitalization rate e_1, followed by the bacterial removal rates μ_E and μ_A. The largest positive indices are associated with environmental transmission to susceptible individuals, β_{E1} and β_{A1}, and with the direct symptomatic transmission coefficient b_1. The equal indices for β_{E1} and β_{A1}, for β_{E2} and β_{A2}, for σ_E and σ_A, and for μ_E and μ_A provide internal checks on the calculation because the corresponding pairs enter $\mathcal{R}_0$ symmetrically at equal baseline values.

These indices are local elasticities around the baseline parameter set and should not be interpreted as a global uncertainty analysis. Within this baseline, reducing direct and environmental transmission and increasing hospitalization or bacterial removal lowers $\mathcal{R}_0$ most effectively among the parameters considered. Figure 4.1 summarizes these indices.

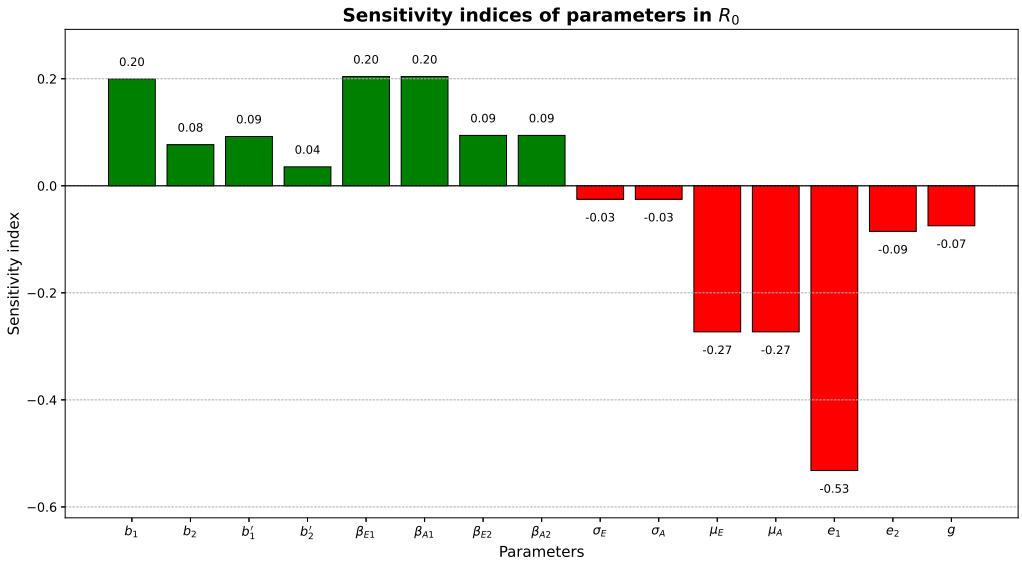


Figure 4.1: Normalized forward sensitivity indices of the selected parameters with respect to $\mathcal{R}_0$ at the common literature-informed baseline.

5. Graphical Analysis and Discussion

To investigate the dynamical behavior of the proposed Caputo–Fabrizio fractional-order typhoid fever model, we use the initialized explicit quadrature scheme described below. The numerical simulations are performed for different values of the fractional order α in order to illustrate the influence of memory effects on the disease dynamics. The considered fractional orders are

$$\alpha = 0.55,\ 0.60,\ 0.65,\ 0.70,\ 0.75,\ 0.80,\ 0.85,\ 0.90,\ 0.92,\ 0.95,\ 0.98,\ 1.$$

The case $\alpha = 1$ corresponds to the classical integer-order model, while $0 < \alpha < 1$ represents the fractional-order system with memory effects.

Consistently with the initialized formulation used in the analysis, for

$${}^{CF}D_t^{\alpha} X(t) = F(t, X(t))$$

we use

$$X(t) = X_0 + (1-\alpha)\big[F(t, X(t)) - F(0, X_0)\big] + \alpha \int_0^t F(y, X(y))\, dy. \tag{5.1}$$

On the uniform grid $t_k = kh$, this gives the explicit quadrature rule

$$X_{k+1} = X_0 + (1-\alpha)\big[F(t_k, X_k) - F(t_0, X_0)\big] + \alpha h \sum_{m=0}^{k} F(t_m, X_m). \tag{5.2}$$

The numerical simulations below use $h = 0.1$ day on $0 \le t \le 80$ days. Componentwise,

$$X_{i,k+1} = X_{i,0} + (1-\alpha)\big[F_i(t_k, X_k) - F_i(t_0, X_0)\big] + \alpha h \sum_{m=0}^{k} F_i(t_m, X_m), \qquad i = 1, \dots, 8.$$

Figures 5.1–5.3 display the trajectories obtained with this initialized scheme.

To assess the numerical robustness with respect to the time step, a refinement study was performed with $h = 0.1$, 0.05, and 0.025 day. For two consecutive step sizes, we define the maximum componentwise relative discrepancy on the common grid by

$$E_{h,h/2} = \max_{1 \le j \le 8} \frac{\max_k \left| X_j^{(h)}(t_k) - X_j^{(h/2)}(t_k) \right|}{\max_k \left| X_j^{(h/2)}(t_k) \right|}. \tag{5.3}$$

The results are summarized in Table 5.1. The discrepancy decreases systematically when the time step is halved. Moreover, the ratio $E_{0.1,0.05}/E_{0.05,0.025}$ is close to 2 for all representative fractional orders, which is consistent with approximately first-order numerical behavior. The qualitative trajectories are unchanged under refinement and no numerical oscillations are observed.

Table 5.1: Time-step refinement for the initialized Caputo–Fabrizio quadrature scheme.

α	$E_{0.1,0.05}$	$E_{0.05,0.025}$	Ratio
0.55	1.903×10^{-3}	9.423×10^{-4}	2.020
0.70	2.450×10^{-3}	1.211×10^{-3}	2.023
0.90	3.310×10^{-3}	1.633×10^{-3}	2.027
1.00	3.831×10^{-3}	1.889×10^{-3}	2.028

The numerical simulations use the same literature-informed demographic baseline adopted in the sensitivity analysis. Specifically, the Taiwan population scale and natural mortality reported by Alharbi et al. [25] give

$$\Pi_1 = 795.592 \text{ persons/day}, \qquad \mu_1 = 3.42081 \times 10^{-5} \text{ day}^{-1},$$

so that $\Pi_1/\mu_1 \approx 2.32574 \times 10^7$ persons. For the numerical baseline we set $\theta_i = 0$, $i = 1, \ldots, 5$, corresponding to a closed reference scenario without exogenous immigration. This avoids treating the large approximate immigration inflows used in the source deterministic simulations as calibrated Taiwan data. The transmission coefficients for vaccinated susceptible individuals are reduced using the vaccine efficacy $\varepsilon_v = 0.75$ reported by Alharbi et al. [25]:

$$b'_j = (1 - \varepsilon_v) b_j, \quad j = 1, 2, \qquad \beta_{E2} = (1 - \varepsilon_v)\beta_{E1}, \qquad \beta_{A2} = (1 - \varepsilon_v)\beta_{A1}.$$

Thus $b'_1 = b'_2 = 2.5 \times 10^{-9}$ and $\beta_{E2} = \beta_{A2} = 2.5 \times 10^{-10}$. The remaining transition and environmental rates are taken from, or based on the baseline values reported by Oubouskour et al. [27]; values identified there as approximate are explicitly marked below. The simulations are qualitative and are not presented as a statistical calibration of the present fractional model.

To avoid interpreting millions of infected individuals as observed typhoid prevalence, the initial state is chosen as a small perturbation of the Taiwan-sized disease-free demographic partition. The susceptible and vaccinated classes are adjusted so that the initial human total remains approximately Π_1/μ_1, while the infected compartments contain only a small illustrative seed. The order of magnitude of this seed is comparable to the low-count initialization used in the Taiwan fitting study of Alharbi et al. [25], but the present initial state is not fitted to incidence data.

The units in Table 5.3 are stated according to the dimensional role of each term in system (3.1): demographic inflows are measured in persons/day, transition and removal coefficients in day^{-1}, direct mass-action transmission coefficients in person^{-1} day^{-1}, and environmental transmission/shedding coefficients relative to the scaled bacterial-load unit. This dimensional convention also makes clear why E_n should be interpreted as a scaled environmental load rather than as a measured concentration without an explicit sampling volume.

Table 5.2: Initial conditions used in the numerical simulations under the literature-informed low-prevalence baseline.

Variable	Value	Unit	Interpretation/status
$S(0)$	8,168,607	persons	DFE-scale susceptible population
$S_v(0)$	15,088,651	persons	DFE-scale vaccinated population
$E(0)$	100	persons	illustrative low-prevalence seed
$I_S(0)$	33	persons	illustrative low-prevalence seed
$I_A(0)$	20	persons	illustrative low-prevalence seed
$H(0)$	0	persons	no initial hospitalization
$R(0)$	5	persons	illustrative recovered seed
$E_n(0)$	2000	scaled load units	illustrative environmental load

Table 5.3: Parameter values, units, and source/status used in the numerical simulations.

Parameter	Value	Unit	Source/status
f_1, f_2	0.01	day^{-1}	Oubouskour et al. [27]
δ	0.054	day^{-1}	Oubouskour et al. [27]
ξ_{A1}, ξ_{E1}	0.78	load unit person^{-1} day^{-1}	Oubouskour et al. [27]
ξ_{A2}, ξ_{E2}	0.05	load unit person^{-1} day^{-1}	Oubouskour et al. [27]; approximate baseline

Parameter	Value	Unit	Source/status
c_1	0.008	day^{-1}	Oubouskour et al. [27]; approximate baseline
c_2	0.0635	day^{-1}	Oubouskour et al. [27]
e_1, e_2	0.375, 0.064	day^{-1}	Oubouskour et al. [27]
d_1, d_2	0.3402, 0.0378	day^{-1}	Oubouskour et al. [27]
d_3	0.1	day^{-1}	Oubouskour et al. [27]; approximate baseline
g	0.0512	day^{-1}	Oubouskour et al. [27]; approximate baseline
b_1, b_2	1.0×10^{-8}	person^{-1} day^{-1}	Oubouskour et al. [27]
ε_v	0.75	dimensionless	Alharbi et al. [25]
b_1', b_2'	2.5×10^{-9}	person^{-1} day^{-1}	derived as $(1-\varepsilon_v)b_j$
β_{A1}, β_{E1}	1.0×10^{-9}	load-unit^{-1} day^{-1}	Oubouskour et al. [27]
β_{A2}, β_{E2}	2.5×10^{-10}	load-unit^{-1} day^{-1}	derived as $(1-\varepsilon_v)\beta_{A1,E1}$
a_1	0.054	day^{-1}	Alharbi et al. [25]
a_2	0.0292	day^{-1}	Alharbi et al. [25]
μ_1	3.42081×10^{-5}	day^{-1}	Alharbi et al. [25]
μ_2, μ_3	0.079	day^{-1}	Oubouskour et al. [27]
μ_E, μ_A	0.1085	day^{-1}	Oubouskour et al. [27]
σ_E, σ_A	0.01	day^{-1}	Oubouskour et al. [27]; approximate baseline
$\lambda_i,\ i = 1, \ldots, 4$	0.001868	day^{-1}	Oubouskour et al. [27]; approximate baseline
Π_1	795.592	persons day^{-1}	Alharbi et al. [25]
$\theta_i,\ i = 1, \ldots, 5$	0	persons day^{-1}	closed numerical reference scenario

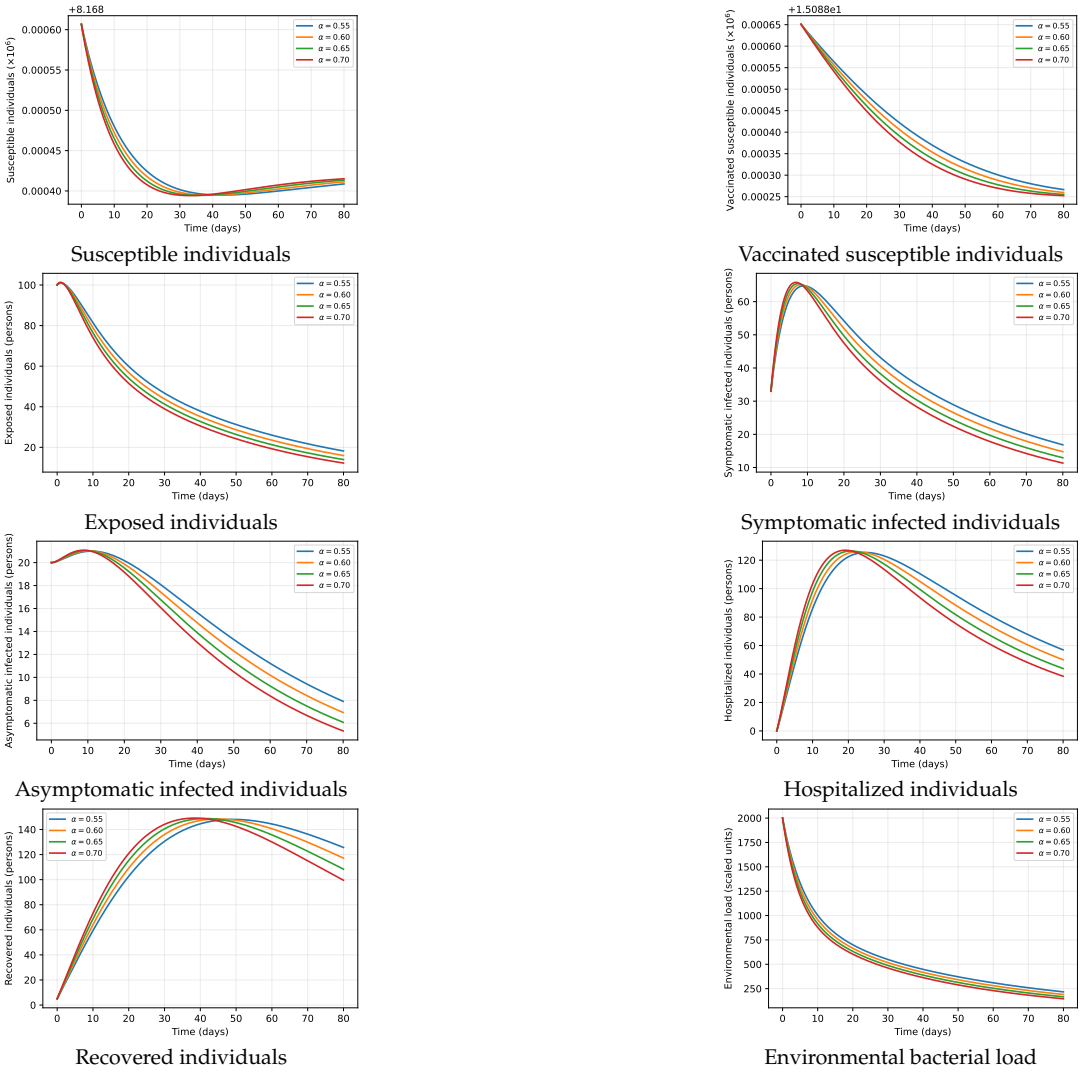


Figure 5.1: Dynamics of the typhoid fever compartments for $\alpha = 0.55, 0.60, 0.65, 0.70$ using the Caputo–Fabrizio fractional derivative.

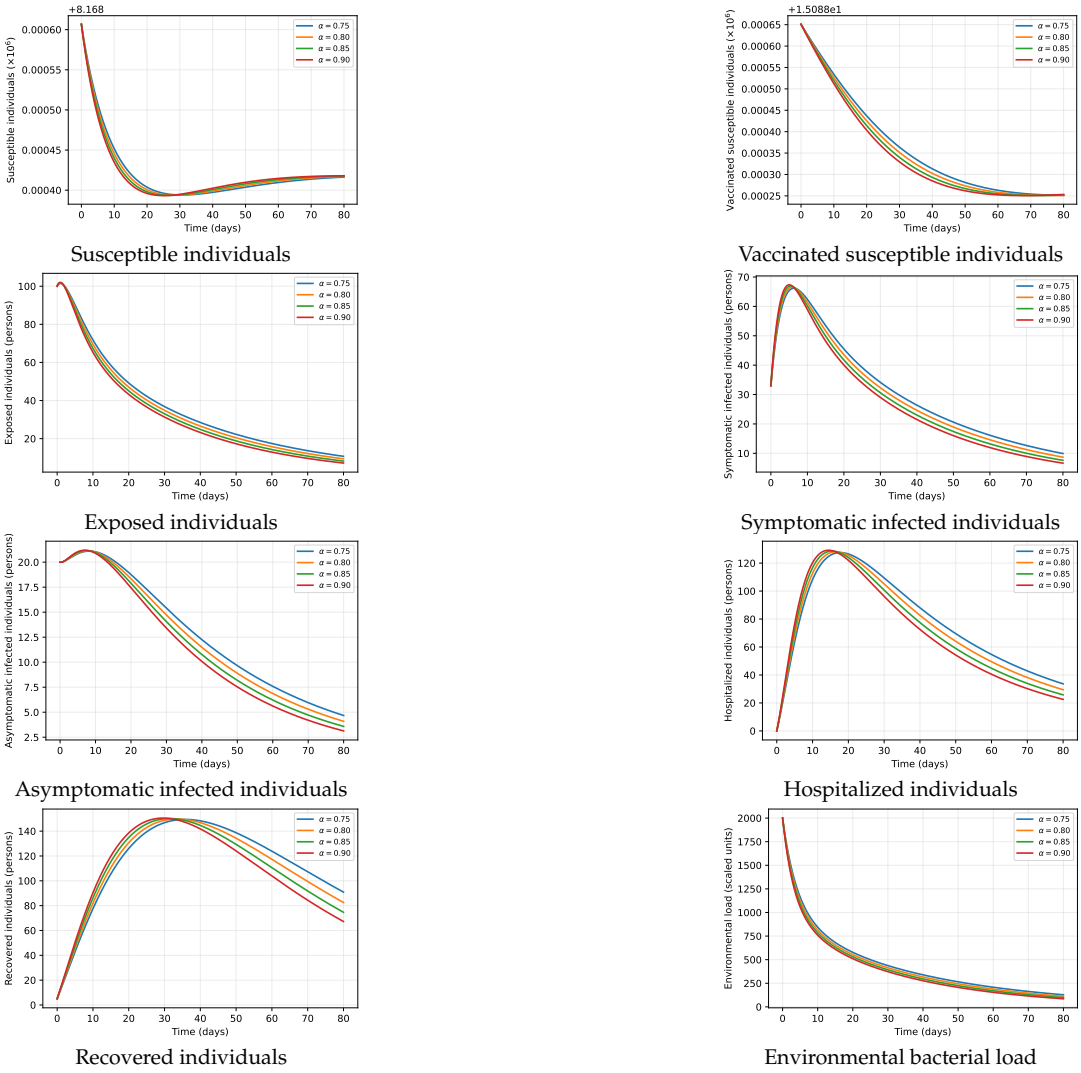


Figure 5.2: Dynamics of the typhoid fever compartments for $\alpha = 0.75, 0.80, 0.85, 0.90$ using the Caputo–Fabrizio fractional derivative.

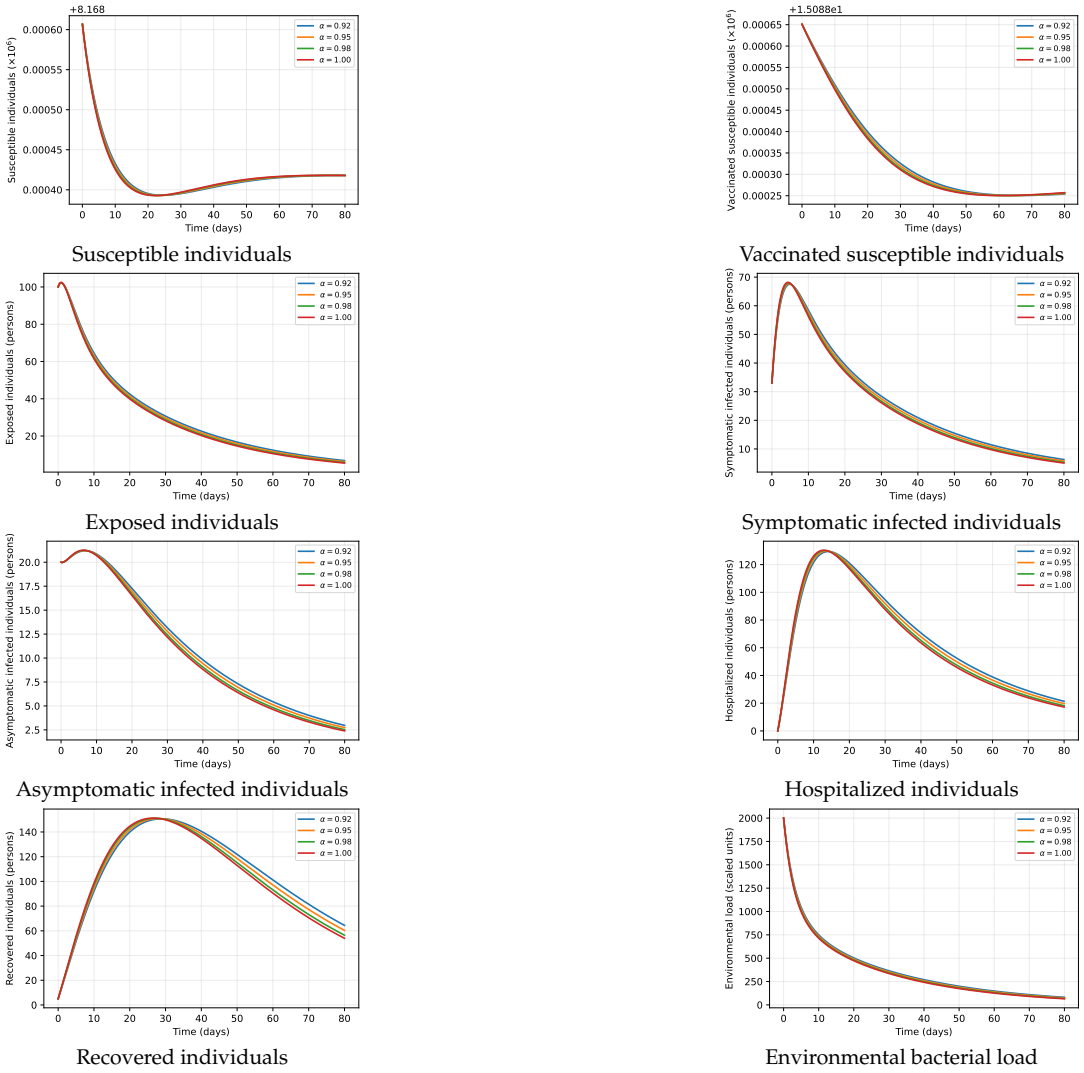


Figure 5.3: Dynamics of the typhoid fever compartments for $\alpha = 0.92, 0.95, 0.98, 1.00$ using the Caputo–Fabrizio fractional derivative.

Figures 5.1–5.3 illustrate the dynamical behavior of the proposed Caputo–Fabrizio fractional-order typhoid fever model for different values of the fractional order α. The numerical results show that the fractional order changes the transient evolution of the epidemiological compartments. In addition to the visual comparison, Table 5.4 reports selected peak and final values for the most epidemiologically relevant compartments. These values should be interpreted as model-based numerical indicators obtained with the parameter set used in the simulations.

Table 5.4: Selected numerical indicators obtained with the initialized Caputo–Fabrizio scheme and the literature-informed low-prevalence baseline. Human compartments are reported in persons; E_n is reported in scaled load units.

α	$E_{\max}$	t_E	$I_{S,\max}$	t_{I_S}	$I_A(80)$	$H_{\max}$	t_H	$E_n(80)$
0.55	100.88	1.0	64.78	9.0	7.91	125.41	24.8	216.87
0.70	101.30	1.0	65.81	6.8	5.33	126.99	19.1	146.03
0.90	102.03	0.9	67.33	5.0	3.13	129.21	14.5	85.70
1.00	102.47	0.8	68.17	4.4	2.39	130.36	12.8	65.47

For the literature-informed baseline, the infected classes remain at low absolute levels relative to the Taiwan-sized human population. The exposed class shows only a small early increase, while the symptomatic

and hospitalized classes exhibit transient peaks and then decline. The environmental bacterial load decreases from its initial value of 2000 scaled units. Increasing α from 0.55 to 1.00 shifts the symptomatic peak earlier (from about day 9.0 to day 4.4) and reduces the residual environmental load at day 80 (from about 216.87 to 65.47 scaled units). Smaller fractional orders therefore produce a more persistent transient in this baseline, whereas the integer-order limit relaxes more rapidly after the initial perturbation.

These comparisons show that changing the fractional order changes the transient trajectories produced by the model. They do not establish that a particular fractional order gives a better fit to observed typhoid data. The initial disease burden is an illustrative low-prevalence perturbation and the parameter set is literature-informed rather than statistically estimated for the present fractional system. The simulations are therefore interpreted as qualitative model-based outputs, not as a calibrated forecast.

6. Conclusion

This paper developed a Caputo–Fabrizio fractional-order model for typhoid fever transmission with environmental contamination. The model extends a recent deterministic typhoid framework by introducing a non-singular fractional memory kernel, while preserving key biological mechanisms such as vaccination, symptomatic and asymptomatic infection, hospitalization, recovery, immigration, and bacterial persistence in contaminated water and food. Positivity and boundedness of the solutions were established, and the biologically feasible region was shown to be positively invariant. The existence and uniqueness of solutions were proved using a fixed-point argument based on the Caputo–Fabrizio integral representation. The disease-free equilibrium and the basic reproduction number were derived, and sensitivity analysis identified the transmission and environmental parameters that most strongly affect $\mathcal{R}_0$. Numerical simulations demonstrated that changing the fractional order modifies the transient evolution of the exposed, infected, hospitalized, recovered, and environmental bacteria compartments.

The numerical differences observed between fractional orders should not be interpreted as showing that the Caputo–Fabrizio formulation fits typhoid data better than the integer-order model. The present fractional system was not statistically calibrated or independently validated against an epidemiological dataset; consequently, the simulations establish sensitivity of transient model behavior to α, not superior predictive performance. The study also has structural limitations: the endemic equilibrium was characterized as a positive solution of the steady-state system, but a complete proof of uniqueness was not established, and several numerical parameters remain literature-informed or approximate rather than estimated for the present model. Future work should therefore include rigorous endemic-equilibrium analysis, parameter estimation and identifiability from epidemiological data, uncertainty quantification, out-of-sample validation, and only then a quantitative comparison between fractional and integer-order formulations. Spatial heterogeneity and optimal control are also natural extensions.

References

[1] U. Baig, S. M. Mehdi, and N. Iftikhar, A pattern of antibiotic drug resistance of *Salmonella* Typhi and *Salmonella* Paratyphi among children with enteric fever in a tertiary care hospital in Lahore, Pakistan, *Croatian Medical Journal*, 64(4), 256, 2023. View online.

[2] Z. A. Bhutta, Current concepts in the diagnosis and treatment of typhoid fever, *BMJ*, 333(7558), 78–82, 2006. View online.

[3] Centers for Disease Control and Prevention, Typhoid Fever and Paratyphoid Fever, Available at: https://www.cdc.gov/typhoid-fever/index.html, Accessed: 01-06-2023.

[4] J. Farrar, P. J. Hotez, T. Junghanss, G. Kang, D. Lalloo, N. J. White, and P. J. Garcia, *Manson's Tropical Diseases*, Elsevier Health Sciences, 2023.

[5] M. S. Bronze and R. A. Greenfield, *Biodefense: Principles and Pathogens*, Horizon Bioscience, Wymondham, Norfolk, England, 2005. View online.

[6] Government of Canada, *Salmonella enterica*, Available at: https://www.canada.ca/, Accessed: 27-10-2023.

[7] C. H. Watson and W. J. Edmunds, A review of typhoid fever transmission dynamic models and economic evaluations of vaccination, *Vaccine*, 33, C42–C54, 2015. View online.

[8] Institut Pasteur, Salmonellosis, Available at: https://www.pasteur.fr/fr/centre-medical/fiches-maladies/salmonellose, Accessed: 27-10-2023.

[9] J. D. Stanaway, R. C. Reiner, B. F. Blacker, E. M. Goldberg, I. A. Khalil, C. E. Troeger, J. R. Andrews, Z. A. Bhutta, J. A. Crump, J. Im, and F. Marks, The global burden of typhoid and paratyphoid fevers: A systematic analysis for the Global Burden of Disease Study 2017, *The Lancet Infectious Diseases*, 19(4), 369–381, 2019. View online.

[10] D. Piovani, G. Figlioli, G. K. Nikolopoulos, and S. Bonovas, The global burden of enteric fever, 2017–2021: A systematic analysis from the Global Burden of Disease Study 2021, *EClinicalMedicine*, 77, 2024. View online.

[11] S. H. Mirza, N. J. Beeching, and C. A. Hart, Multi-drug resistant typhoid: A global problem, *Journal of Medical Microbiology*, 44(5), 317–319, 1996. View online.

[12] R. Birger, M. Antillón, J. Bilcke, C. Dolecek, G. Dougan, A. J. Pollard, K. M. Neuzil, I. Frost, R. Laxminarayan, and V. E. Pitzer, Estimating the effect of vaccination on antimicrobial-resistant typhoid fever in 73 countries supported by Gavi: A mathematical modelling study, *The Lancet Infectious Diseases*, 22(5), 679–691, 2022. View online.

[13] World Health Organization, Typhoid vaccines: WHO position paper, *Weekly Epidemiological Record*, 93(13), 153–172, 2018. View online.

[14] J. González-Guzmán, An epidemiological model for direct and indirect transmission of typhoid fever, *Mathematical Biosciences*, 96(1), 33–46, 1989. View online.

[15] J. W. Karunditu, G. Kimathi, and S. Osman, Mathematical modeling of typhoid fever disease incorporating unprotected humans in the spread dynamics, *Journal of Advances in Mathematics and Computer Science*, 32(3), 1–11, 2019. View online.

[16] J. M. Mutua, F. B. Wang, and N. K. Vaidya, Modeling malaria and typhoid fever co-infection dynamics, *Mathematical Biosciences*, 264, 128–144, 2015. View online.

[17] A. S. Shaikh and K. S. Nisar, Transmission dynamics of fractional order typhoid fever model using Caputo–Fabrizio operator, *Chaos, Solitons and Fractals*, 128, 355–365, 2019. View online.

[18] S. Mushayabasa, A simple epidemiological model for typhoid with saturated incidence rate and treatment effect, *International Journal of Mathematical and Computational Sciences*, 6(6), 688–695, 2013.

[19] S. Mushayabasa, Modeling the impact of optimal screening on typhoid dynamics, *International Journal of Dynamics and Control*, 4, 330–338, 2016. View online.

[20] J. Mondal, Influence of awareness programs by media in the typhoid fever: A study based on mathematical modeling, *Journal of Mathematical Modeling*, 6(1), 1–26, 2018. View online.

[21] S. S. Musa, S. Zhao, N. Hussaini, S. Usaini, and D. He, Dynamics analysis of typhoid fever with public health education programs and final epidemic size relation, *Results in Applied Mathematics*, 10, 100153, 2021. View online.

[22] O. J. Peter, M. O. Ibrahim, H. O. Edogbanya, F. A. Oguntolu, K. Oshinubi, A. A. Ibrahim, T. A. Ayoola, and J. O. Lawal, Direct and indirect transmission of typhoid fever model with optimal control, *Results in Physics*, 27, 104463, 2021. View online.

[23] G. T. Tilahun, O. D. Makinde, and D. Malonza, Modelling and optimal control of typhoid fever disease with cost-effective strategies, *Computational and Mathematical Methods in Medicine*, 2017, 2324518, 2017. View online.

[24] G. T. Tilahun, O. D. Makinde, and D. Malonza, Co-dynamics of pneumonia and typhoid fever diseases with cost effective optimal control analysis, *Applied Mathematics and Computation*, 316, 438–459, 2018. View online.

[25] M. H. Alharbi, F. K. Alalhareth, and M. A. Ibrahim, Analyzing the dynamics of a periodic typhoid fever transmission model with imperfect vaccination, *Mathematics*, 11(15), 3298, 2023. View online.

[26] H. Abboubakar, L. K. Kombou, A. D. Koko, H. P. E. Fouda, and A. Kumar, Projections and fractional dynamics of the typhoid fever: A case study of Mbandjock in the Centre Region of Cameroon, *Chaos, Solitons and Fractals*, 150, 111129, 2021. View online.

[27] K. Oubouskour, S. Khassal, B. Khajji, and O. Balatif, Mathematical modeling and optimal control strategies of the typhoid transmission with cost-effectiveness analysis, *Iranian Journal of Numerical Analysis and Optimization*, 16(1), 304–338, 2026. View online.

[28] I. A. Baba and B. A. Nasidi, Fractional order epidemic model for the dynamics of novel COVID-19, *Alexandria Engineering Journal*, 60(1), 537–548, 2021. View online.

[29] B. S. Alkahtani, Mathematical modeling of COVID-19 transmission using a fractional-order derivative, *Fractal and Fractional*, 7(1), 46, 2022. View online.

[30] S. Mangal, O. P. Misra, and J. Dhar, Modeling the effect of vaccination in fractional-order epidemic model for infectious disease, *International Journal of Dynamics and Control*, 12(1), 303–317, 2024. View online.

[31] M. ur Rahman, S. Ahmad, R. T. Matoog, N. A. Alshehri, and T. Khan, Study on the mathematical modelling of COVID-19 with Caputo–Fabrizio operator, *Chaos, Solitons and Fractals*, 150, 111121, 2021. View online.
[32] D. Yu, X. Liao, and Y. Wang, Modeling and analysis of Caputo–Fabrizio definition-based fractional-order boost converter with inductive loads, *Fractal and Fractional*, 8(2), 81, 2024. View online.
[33] I. Ahmed, C. Kiataramkul, M. Muhammad, and J. Tariboon, Existence and sensitivity analysis of a Caputo fractional-order diphtheria epidemic model, *Mathematics*, 12(13), 2033, 2024. View online.
[34] A. Yusuf, B. Acay, U. T. Mustapha, M. Inc, and D. Baleanu, Mathematical modeling of pine wilt disease with Caputo fractional operator, *Chaos, Solitons and Fractals*, 143, 110569, 2021. View online.
[35] R. Jan, M. A. Khan, P. Kumam, and P. Thounthong, Modeling the transmission of dengue infection through fractional derivatives, *Chaos, Solitons and Fractals*, 127, 189–216, 2019. View online
[36] N. Ullah, Z. Shah, R. Jan, S. Islam, N. Vrinceanu, M. Farhan, and E. Antonescu, Existence and sensitivity analysis of a Caputo–Fabrizio fractional order vector-borne disease model, *European Journal of Pure and Applied Mathematics*, 18(2), Article 5687, 2025. View online.
[37] S. G. Kebede and A. G. Lakoud, Analysis of mathematical model involving nonlinear systems of Caputo–Fabrizio fractional differential equation, *Boundary Value Problems*, 2023, Article 44, 2023. View online.
[38] S. Rezapour, S. Etemad, and H. Mohammadi, A mathematical analysis of a system of Caputo–Fabrizio fractional differential equations for the anthrax disease model in animals, *Advances in Difference Equations*, 2020, Article 481, 2020. View online.
[39] H. Li, J. Cheng, H.-B. Li, and S.-M. Zhong, Stability analysis of a fractional-order linear system described by the Caputo–Fabrizio derivative, *Mathematics*, 7(2), 200, 2019. View online.
[40] M. Caputo and M. Fabrizio, A new definition of fractional derivative without singular kernel, *Progress in Fractional Differentiation and Applications*, 1(2), 73–85, 2015. View online.
[41] J. Losada and J. J. Nieto, Properties of a new fractional derivative without singular kernel, *Progress in Fractional Differentiation and Applications*, 1(2), 87–92, 2015. View online.

Citation IEEE Format:
E. Nafia, A. Es-sallamy, and M. E. Omari *"A Caputo–Fabrizio Fractional-Order Typhoid Fever Model with Environmental Transmission and Sensitivity Analysis"*, *Jurnal Diferensial*, vol. 8(2), pp. 219-241, 2026.

This work is licensed under a Creative Commons "Attribution-ShareAlike 4.0 International" license.

